*Int. J. Multiphase Flow* Vol. 12, No. 6, pp. 997–1007, 1986
Printed in Great Britain

0301-9322/86 $3.00 + 0.00
Pergamon Journals/Elsevier

# NUMERICAL TREATMENT OF THE STEADY FLOW OF A LIQUID COMPOUND JET

S. RADEV and P. GOSPODINOV
Institute of Mechanics and Biomechanics, Bulgarian Academy of Sciences,
P.O. Box 373, 1090 Sofia, Bulgaria

(*Received* 4 *March* 1985; *in revised form* 14 *October* 1985)

**Abstract**—A numerical treatment of the outflow of a two-layer laminar jet into a non-viscous continuous phase is performed. The dispersed phases (i.e. the central core and the concentric layer) are immiscible, incompressible and Newtonian fluids. The method of solution allows for the simultaneous determination of the shape of both interfaces, as well as of the corresponding velocity profiles. The equations of motion of both phases are obtained in a boundary layer approximation. The pressure jump in the radial direction, owing to forces of interfacial tension, is taken into account. Also studied is how the initial velocity profiles at the nozzle exit and some dimensionless parameters affect the interaction between the primary and secondary flow. Numerical results agree qualitatively with some experimental evidence. The approach can also be employed to predict the flow within a viscous continuous phase.

## 1. INTRODUCTION

Compound jets have recently become of essential interest, and what seems worth trying is to describe some methods for their generation. A method of practical use, however, has been proposed by Hertz & Hermanrud (1983), where a liquid jet is ejected through a layer of immiscible liquid. After breaking the free surface, the primary jet flows out surrounded by a sheath of the immiscible fluid, and the secondary jet thus obtained becomes accelerated by the primary one. Such flow is usually employed in ink-jet printing, granulators etc. The advantage of the compound jet flow exists in its capability to produce drops surrounded by a concentric surface layer of prescribed properties. Moreover, the second layer exercises control over both the instability and drop size of the primary jet.

Similar to the one-layer jet, the compound jet flow is time dependent and unstable. Following the classical approach of linear stability theory, we will consider the jet flow to be a superposition of a non-disturbed (steady) flow and a perturbed (unsteady) one. The present paper studies the steady laminar flow of an axisymmetric compound jet. The equations of motion of the primary and the concentric jets, as well as the boundary conditions at the interface surface, are written in a boundary layer approximation that was adopted by Gospodinov *et al.* (1979), but for a one-layer jet. The numerical method proposed in that work is extended to the study of the flow of a compound jet. Numerical results for the jet velocity profiles, the radii of both the primary and secondary jets etc. are obtained.

## 2. FORMULATION OF THE PROBLEM

Consider an axisymmetric compound jet with axis $Oz$ (figure 1) directed vertically. Let the jet consist of two immiscible, viscous and incompressible liquids of densities $\rho_j$ and viscosities $\mu_j$. Furthermore, let $j = 1$ for the central core of the jet and $j = 2$ for its concentric part. We will use the index 3 to denote the parameters of the surrounding medium when necessary. For reasons of simplicity the latter is treated as a non-viscous gas at rest of density $\rho_3$ and pressure $p_3$. However, there are no principal difficulties in incorporating the viscosity of the surrounding medium. To avoid difficulties during the analysis of the initial zone of the configuration, given by Hertz & Hermanrud (1983), simpler ways of producing a compound jet are employed. Suppose that the liquids flow

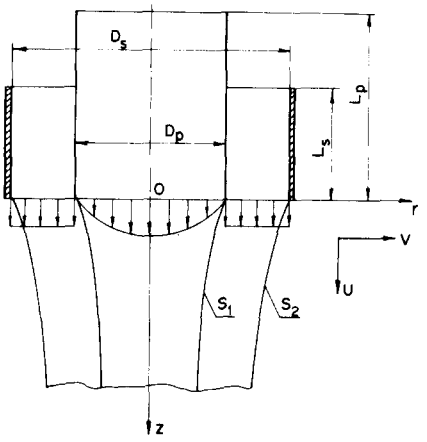


Figure 1. Flow configuration.

out of a nozzle with flow rates $Q_j$ and that the nozzle consists of two cylindric pipes with axis $Oz$ (cross-sections are circular with diameters $D_P$ and $D_S$, respectively). Let us denote by $u_P$ and $u_S$ the corresponding mean outflow velocities of the central core and of the jet sheath part.

As was noted, the flow of the compound jet will be considered to be laminar and steady. Two interfaces are observed within the flow, their equations reading

$$r = H_j. \qquad [1]$$

Considering the steady case, they can be treated as stream surfaces and can be obtained by solving the differential equation

$$U_j \frac{dH_j}{dz} = V_j, r = H_j \ (j = 1, 2), \qquad [2]$$

where $(U_j, V_j)$ are the axial and radial components of the flow velocity.

Although an additional concentric jet has been taken into account, it is clear that the flow behaviour of the compound jet is similar to that of the one-layer one.

It has to be noted that the equations of motion, written by employing a boundary layer approximation and valid for a single liquid jet outflowing in a non-viscous gas, have been obtained by Duda & Vrentas (1967). If viscosity of the continuous phase is taken into account, then the equations of flow of a capillary jet in immiscible liquid–liquid systems are obtained (see Yu & Sheele 1975). This flow, however, was treated by Gospodinov *et al.* (1979) by employing a boundary layer approximation, whereas appropriate estimates of the order of magnitude of the flow parameters were adopted. When considering a compound jet flow, such an approach allows one to disregard the pressure variation $P_j$ across the jet. This and some other simplifications hold because the flow parameters vary very slowly in the axial direction. As shown by Gospodinov *et al.* (1979), the boundary layer approximation of both the equations of motion and continuity has the form

$$U_j \frac{\partial U_j}{\partial z} + V_j \frac{\partial U_j}{\partial r} = \frac{2}{\mathrm{Re}} \frac{\mu_j}{\mu_1} \frac{\rho_1}{\rho_j} \frac{1}{r} \frac{\partial}{\partial r} \left( r \frac{\partial U_j}{\partial r} \right) + F_j, \qquad [3]$$

$$\frac{\partial}{\partial z}(rU_j) + \frac{\partial}{\partial r}(rV_j) = 0 \qquad [4]$$

and

$$\frac{\partial P_j}{\partial r} = 0 \quad (j = 1, 2), \qquad [5]$$

where

$$F_j = \frac{1}{2\mathrm{Fr}} - \frac{\rho_1}{\rho_j}\frac{\partial P_j}{\partial z}.$$

The above equations have to be applied to both the primary and secondary jet flows. However, non-dimensional quantities appear in [3]–[5] and the following scales have to be introduced: $D_P/2$ for distance, $u_P$ for velocity and $\rho_1 u_P^2$ for pressure. Since a second fluid is present, new parameters together with the Froude number ($\mathrm{Fr} = u_P^2/gD_P$) as well as the Reynolds number ($\mathrm{Re} = \rho_1 D_P u_P/\mu_1$) of the primary jet can appear in the equations. Such, for instance, are the density non-dimensional ratio $\rho_2/\rho_1$ and the viscosity ratio $\mu_2/\mu_1$. The Froude number with $g$ as gravity acceleration (see [3]) accounts for the gravity forces.

Equations [3]–[5] are to be applied to a flow of very complicated geometry, i.e. bounded by the symmetry axis of the primary jet, as well as by two interfaces $S_j$. Therefore, it seems necessary to complete the equations with additional conditions. The latter, however, are to describe physically the flow behaviour at the separated surfaces. The symmetry condition is to be written in the form

$$V_1 = 0 \qquad [6]$$

and

$$\frac{\partial U_1}{\partial r} = 0. \qquad [7]$$

Two groups of boundary conditions have to be satisfied at the interfaces ($r = H_j$). They interpret physically the interaction between the phases at both sides of the interface. The first group of boundary equations express the balance of tangential and normal stresses at the interface. Below they are written in a non-dimensional form, employing a boundary layer approximation:

$$\frac{\mu_{j+1}}{\mu_1}\frac{\partial U_{j+1}}{\partial r} - \frac{\mu_j}{\mu_1}\frac{\partial U_j}{\partial r} = 0 \qquad [8]$$

and

$$P_{j+1} - P_j = -\frac{2}{\mathrm{We}}\frac{\sigma_j}{\sigma_1}H_j^{-1} \quad (j = 1, 2). \qquad [9]$$

Equation [9] calculates the difference in pressure on both sides of each interface, as balanced by the surface tension. However, these conditions provide two new dimensionless parameters, i.e. the Weber number ($\mathrm{We} = \rho_1 D_P u_P^2/\sigma_1$) of the primary jet and the ratio of the surface tension coefficients $\sigma_j$ of the interfaces $S_j$. Equation [8] gives the discontinuity of the axial velocity profile, owing to the difference between the viscosity coefficients of the liquids. It can be simplified for the outside surface $S_2$ by considering the surrounding non-viscous gas $\mu_3 = 0$.

Two additional conditions that are to be satisfied at the interface are obtained from the second group of boundary conditions. The form of the first one is that of a non-slip condition for the axial velocities,

$$U_1 = U_2, \quad r = H_1, \qquad [10]$$

and is to be applied only to the inside surface $S_1$. The second one, however, is a condition for zero mass flux through the interfaces. It has already been used in the form [2], when accounting for the surface of the primary jet and the outside surface of the concentric jet. A zero mass flux condition at the inner surface of the concentric jet is also to be satisfied. It seems convenient to write it in an equivalent form:

$$V_1 = V_2, \quad r = H_1. \qquad [11]$$

Note that [10] and [11] provide the equality between the tangential and normal velocity components.

Thus, the mathematical description of the flow of a liquid compound jet is fulfilled. It consists of a system of four partial second-order differential equations, [3] and [4], completed by a set of boundary conditions, [6]–[11], along the jet axis $r = 0$ and at the interfaces $S_j$, respectively. However, the equations of the interface surfaces are not known in advance and are to be determined together with the rest of the unknown flow parameters by means of [2]. At the same time, they express the flow surfaces where parameters in different regions are to be put into agreement by satisfying the boundary conditions. This poses the main difficulties of the problem. In what follows a numerical solution is sought.

To determine completely the compound jet flow, the outflow velocity profile must be prescribed at the nozzle exit:

$$U_j = U_{N_j} \quad (j = 1, 2). \tag{12}$$

Furthermore, to characterize the concentric jet flow, the dimensionless ratios of the average velocities of the outflow and the radii of both jets must be given together with the initial profile. These ratios are denoted by

$$U_S = \frac{u_S}{u_P} \quad \text{and} \quad R_S = \frac{D_S}{D_P}. \tag{13}$$

Equation [12] serves as initial velocity profiles for the primary and concentric jets. Usually,

$$V_j = 0 \quad (j = 1, 2) \tag{14}$$

for nozzles of practical use.

It seems more convenient to eliminate initially the pressure term in the equation of motion [3]. To do this, an equation of the outside pressure distribution $P_3$ has to be incorporated:

$$\frac{\partial P_3}{\partial z} = \frac{1}{2\mathrm{Fr}} \frac{\rho_3}{\rho_1}. \tag{15}$$

Equation [15] corresponds to the hydrostatic pressure distribution within the surrounding gaseous phase. With [5] in mind, the axial pressure gradients $\partial P_j/\partial z$ can easily be found from [9] and [15]. Then the $F_j$ terms in [3] are in the form

$$F_2 = \left(1 - \frac{\rho_3}{\rho_2}\right) \frac{1}{2\mathrm{Fr}} + \frac{2}{\mathrm{We}} \frac{\sigma_2}{\sigma_1} H_2^{-2} \frac{\mathrm{d}H_2}{\mathrm{d}z} \tag{16}$$

and

$$F_1 = \left(1 - \frac{\rho_3}{\rho_1}\right) \frac{1}{2\mathrm{Fr}} + \frac{2}{\mathrm{We}} \left(\frac{\sigma_2}{\sigma_1} H_2^{-2} \frac{\mathrm{d}H_2}{\mathrm{d}z} + H_1^{-2} \frac{\mathrm{d}H_1}{\mathrm{d}z}\right). \tag{17}$$

The first term on the r.h.s. of [16] and [17] accounts for the buoyancy effect of the primary and concentric jet flows, respectively, while the second term accounts for the effects of surface tension. A new dimensionless parameter $\rho_3/\rho_2$ appears in [16], but it can be expressed as a product of the ratios that have already been introduced:

$$\frac{\rho_3}{\rho_2} = \frac{\rho_3}{\rho_1} \left(\frac{\rho_2}{\rho_1}\right)^{-1}.$$

## 3. NUMERICAL METHOD

The equations, obtained by using a boundary layer approximation for each of the fluids and completed by taking into account the conditions of both outflow and phase interaction, are to be solved numerically. The numerical method adopted is similar to that employed by Gospodinov *et al.* (1979), but is somewhat improved, as shown by Gospodinov *et al.* (1981). In what follows, its most important aspects are revealed.

A new independent variable is introduced for each of the dispersed phases (instead of the radial coordinate) by using a stream function defined as

$$\psi_1 = \int_0^r xU\,dx, \quad 0 \leqslant r \leqslant H_1(z), \tag{18}$$

and

$$\psi_2 = \int_{H_1}^r xU\,dx, \quad H_1(z) \leqslant r \leqslant H_2(z). \tag{19}$$

Duda & Vrentas (1967) introduced for the first time Protean coordinates to investigate the flow of a single capillary jet. Their idea has been developed in the present study, whereas the stream function is introduced as an independent variable in the equations of motion of both the primary and concentric jets.

It can easily be found (see Gospodinov *et al.* 1979) that the stream function for phase 1 can be normalized as $0 \leqslant \psi_1 \leqslant \frac{1}{2}$. The dimensionless flow rate of phase 2 (i.e. the maximum value of $\psi_2$ in the plane of outflow) is specified as

$$\Psi_2 = \tfrac{1}{2} U_S (R_S^2 - 1). \tag{20}$$

Note that for convenience the inner surface $S_1$ is introduced as a zero streamline of the secondary flow:

$$0 \leqslant \psi_2 \leqslant \Psi_2. \tag{21}$$

It is also convenient to use $\xi = z/\mathrm{Re}$ instead of $z$. By performing a change of the variables, a new unknown function $r(\zeta, \psi)$ is obtained within the equations that describe the flow of both phases, i.e.

$$\frac{\partial r_j^2}{\partial \psi_j} = \frac{2}{U_j} \begin{cases} j = 1, & 0 \leqslant \psi_1 \leqslant \frac{1}{2} \\ j = 2, & 0 \leqslant \psi_2 \leqslant \psi_2 \end{cases}, \tag{22}$$

while the condition along the symmetry axis for $\psi_1 = 0$ is provided by $r_1 = 0$. The condition $r_1 = H_1(\xi)$ holds true, however, for $\psi_1 = \frac{1}{2}$ and $\psi_2 = 0$. Moreover, $r_2 = H_2(\xi)$ is valid for $\psi_2 = \Psi_2$, i.e. at the surface $S_2$. Radii $H_1$ and $H_2$ are obtained naturally by solving [22]. Introducing variables of Protean type, the radial velocity component $V_j$ is determined by solving the equation of the streamlines (see [2]).

$$V_j = U_j \frac{\partial r_j}{\partial \xi} \mathrm{Re}^{-1}. \tag{23}$$

The equations of motion at each knot of the grid are approximated by means of an implicit conservative scheme of second order of accuracy with respect to $\psi_j$. The difference equations thus obtained are combined into a single problem by incorporating the condition of the properly approximated dispersed phase interaction.

The condition along the symmetry axis is employed as in Gospodinov *et al.* (1979). The condition of interaction between the concentric jet and the continuous phase is included in the numerical scheme. However, the latter is written by employing the same order of approximation as that involved in the motion equations.

Thus a system of linearized algebraic equations with a tridiagonal matrix of coefficients is obtained for each row of the grid and for a fixed value of $\xi$ (i.e. $z$). However, the velocity components in the knots of the row are unknown functions. The coefficients in front of them, as well as the r.h.s., depend on $U$, $V$, $r$, $H_1$ and $H_2$, which implies the employment of an iteration procedure. The values of the unknown functions, included in the coefficients, are taken from the previous iteration. The process proceeds until the previously given accuracy is attained. The $\xi$ increases by $\Delta\xi$ and the calculation proceeds for knots of the next row. The optimal values of the grid steps $\Delta\xi$, $\Delta\psi_1$ and $\Delta\psi_2$ are determined by performing a numerical experiment.

The basic principles of design of the difference equations, of the approximation of [22] and [23], and of the iteration process itself are similar to the idea suggested by Gospodinov

*et al.* (1981). Moreover, the scheme employed for the treatment of a viscous continuous phase, when regarding the problem of outflow of a one-phase capillary jet, can easily be applied to the numerical treatment of a compound jet. As related to the nozzle geometry, i.e. to the ratios $L_P/D_P$ and $L_S/D_S$, the initial outflow profile [12] of phase 1 can be parabolic or plane, while that of phase 2 can be taken as a fully developed flow between two concentric pipes (see Bird *et al.* 1965) or as a plane one. As was noted in section 2, the present considerations involve a plane profile of outflow of phase 2.

## 4. RESULTS

Table 1 presents the flow dimensionless parameters for the cases that have been treated numerically. The system of two dispersed phases, together with the corresponding dimensionless parameters, are in accordance with part of the experiments described by Hertz & Hermanrud (1983). However, all this is done to obtain experimental evidence whenever possible. Since the continuous phase is air in all the cases considered, it is taken to be non-viscous. The calculations performed to control cases 1 and 2 show that the air viscosity does not affect the numerical results. The initial outflow velocity profile $U_{N_1}$ of phase 1 is taken to be parabolic or plane when performing the numerical experiments (see notations 1 and 2 in the last column of table 1). Since the compound jet flows out horizontally in all the cases treated, the effect of the gravity acceleration has been ignored throughout.

Cases 1 and 2 correspond to a system, consisting of (80% $H_2O$ + 20% glycerol without dye), i.e. phase 1/phase 2, whereas the initial flow rates are $Q_P = 36 \times 10^{-9}$ and $Q_S = 115 \times 10^{-9}\,m^3/s$, the average velocity of outflow of phase 1 is $u_P = 8.1$ m/s, $\sigma_1 = 20 \times 10^{-3}$ N/m and $\mu_1 = 1.9 \times 10^{-3}$ N s/m$^2$. Case 3 is obtained from case 2 but it is assumed that the ratio of the average outflow velocity is $U_S = 1$. The main reason that makes the compound jet differ from the one-layer jet is the presence of an additional interface, the stream surface $S_1$, which separates two fluids of different physical properties. But this is not so in cases 1–3, where the fluids from both sides of the stream surface $S_1$ are supposed to be the same, but flowing out with different initial velocity profiles. We proceed to study the interaction of the fluids through $S_1$. To calculate these three cases, we must use $P_2 = P_1$ for surface $S_1$ instead of [9], and employ $\sigma_1$ for surface $S_2$ as the only surface tension coefficient ($\sigma_2/\sigma_1 = 1$). Streamlines for cases 1 and 2 are drawn in figures 2 and 3. It is clear that the change of surface $S_2$ corresponds approximately to the observed change of the surface of a one-layer jet (see Gospodinov *et al.* 1979). A certain deflection of the current lines in the $0 \leqslant r \leqslant H_1$ region can be explained (especially in case 1) by means of the more intensive exchange of momentum, which is due to the form of the initial velocity profiles of phases 1 and 2. This, however, is confirmed by the pattern of the profiles of the axial components (case 1) drawn in figure 4. Moreover, these profiles confirm that the relaxation of the velocity profile is considerably weaker in case 2 (figure 5). The variation of radii $H_1(z)$ and $H_2(z)$ of the surfaces $S_1$ and $S_2$ (case 1) corresponds

Table 1

| Case | Re | We | $\frac{\mu^2}{\mu_1}$ | $\frac{\rho_2}{\rho_1}$ | $\frac{\sigma_2}{\sigma_1}$ | $R_S$ | $U_S$ | |
|---|---|---|---|---|---|---|---|---|
| 1 | 320 | 237.2 | 1 | 1 | 0 | 2.56 | 0.64 | 1 |
| 2 | 320 | 237.2 | 1 | 1 | 0 | 2.56 | 0.64 | 2 |
| 3 | 320 | 237.2 | 1 | 1 | 0 | 1.08 | 1 | 2 |
| 4 | 304 | 94.6 | 1 | 1 | 0.385 | 3.33 | 0.32 | 1 |
| 5 | 304 | 94.6 | 1 | 1 | 0.385 | 3.33 | 0.32 | 2 |
| 6 | 316 | 237.2 | 0.53 | 1 | 3.6 | 2.45 | 0.42 | 1 |
| 7 | 316 | 237.2 | 0.53 | 1 | 3.6 | 2.45 | 0.42 | 2 |
| 8 | 304 | 94.6 | 1 | 1 | 0.278 | 2.05 | 1 | 1 |
| 9 | 304 | 94.6 | 1 | 1 | 0.278 | 2.05 | 1 | 2 |
| 10 | 304 | 94.6 | 1 | 1 | 0.278 | 1.5 | 2.47 | 1 |

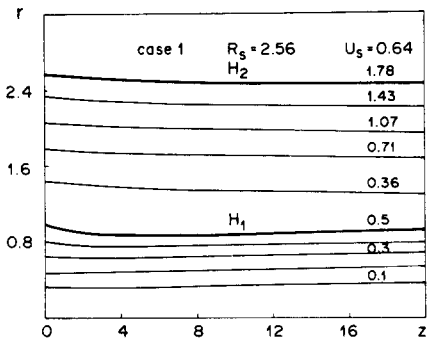


Figure 2. Streamlines.

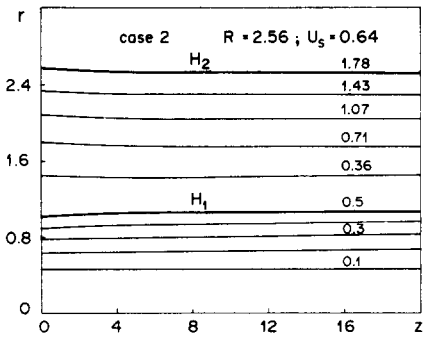


Figure 3. Streamlines.

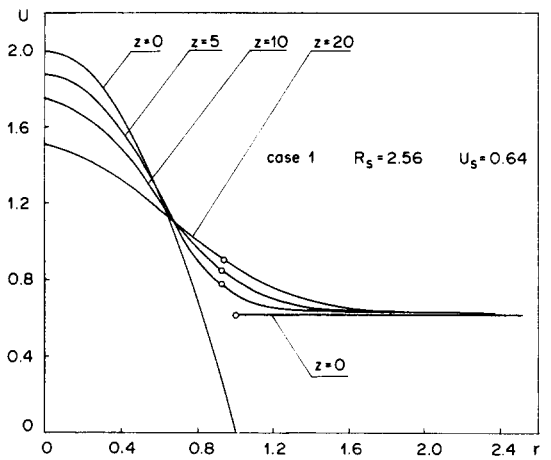


Figure 4. Axial velocity distribution.

qualitatively to the experimental observations of Hertz & Hermanrud (1983). $H_1$ increases for $z > 6$, while $H_2$ decreases, although only slightly, i.e. phase 2 delays phase 1 while phase 1 tends to accelerate phase 2, owing to the exchange of momentum.

The record of the variation of the radial component of velocity $V(r)$, considering three cross-sections along $z$ (figures 6 and 7), confirms our conclusions. Velocity $V$, being zero along the symmetry axis, grows and attains its maximum value in the region of flow of

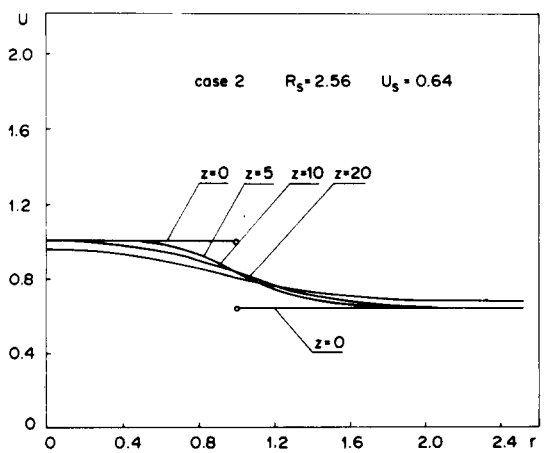


Figure 5. Axial velocity distribution.

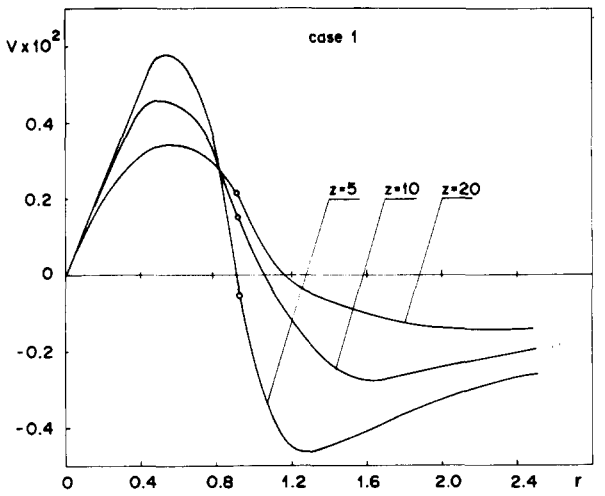


Figure 6. Radial velocity distribution.

phase 1 and $S_1$ expands, although slightly, in both cases. The velocity profile "passes" through zero near the $S_1$ surface, i.e. near the region $r = H_1$. Then it changes sign and attains a local minimum within phase 2. However, $V$ varies slightly near the surface $S_2$. Its value at the surface $S_2$ is finite and negative for $r = H_2$, due to the contraction of the compound jet surface, which is affected by the exchange of momentum, as well as by forces of surface tension. The narrower boundaries of $V(r)$ in case 2 are due to the weaker interaction between the phases.

To test the calculation procedure, we must eliminate entirely the effect of the difference between the initial velocity profiles. Thus we analyse case 3. In fact the latter presents a one-layer capillary jet, flowing horizontally out of a nozzle of dimensionless radius $R_S$. Moreover, the jet's initial profile is homogeneous. As expected, results (not presented graphically) show that the compound jet remains cylindrical while the initial velocity profile does not relax along $z$ and $r$.

The parameters in cases 4 and 5 represent a system consisting of (80% $H_2O$ + glycerol + dye)/(silicon fluid) with $U_P = 8.1$ m/s, $\mu_1 = 2 \times 10^{-3}$ N s/m$^2$, $\sigma_1 = 72 \times 10^{-3}$ and $\sigma_2 = 20 \times 10^{-3}$ N/m, while the initial flow rates are the same as in cases 1–3. What is typical here is that both phases are not the same as in the previous cases and forces of interfacial tension act upon surface $S_1$, while densities and viscosities remain intact.

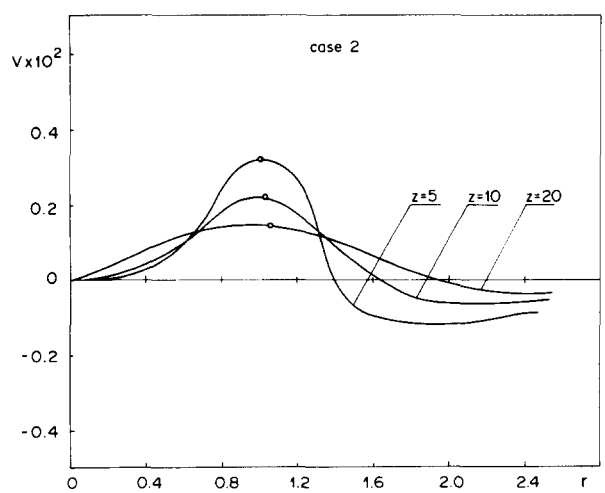


Figure 7. Radial velocity distribution.

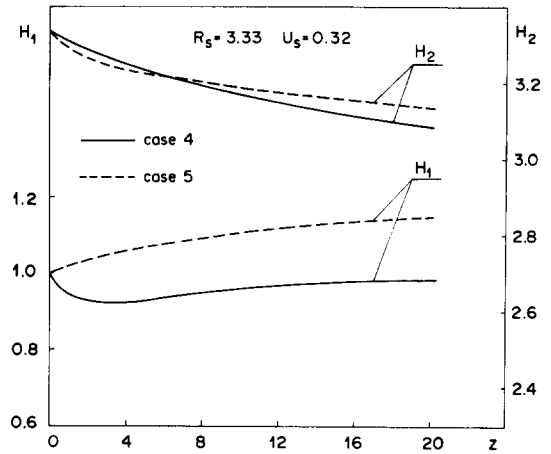


Figure 8. Effect of the initial velocity profiles on the change of radii.

Numerical results show that the change of surface $S_2$ is similar to the change of the surface of a one-layer capillary jet. Radius $H_2$ decreases strongly (figure 8) because the initial outflow velocity $u_S$ is about three times lower than the average initial outflow velocity $u_P$ of phase 1. Hence, the dispersed phase 2 is accelerated considerably downstream. Radius $H_1$ of the internal interface ($z > 4$ in case 5, $z > 0$ in case 4) grows accordingly, owing to the delay that phase 2 exercises on phase 1. Since the $S_1$ surface deflects in the opposite direction, i.e. away from the axis of symmetry, the forces of interfacial tension tend to increase this deflection even more. However, forces of interfacial tension between the viscous phase 2 and the air act upon surface $S_2$, as in the case of a one-layer jet.

What has already been stated is valid for cases 4 and 5 as well, but there still exists a certain difference in the change of $H_1$ (i.e. contraction for $0 \leqslant z \leqslant 4$) which can be explained (as in case 1) by the difference between velocity profiles for case 1, which induce intensive exchange of momentum through the surface. There occurs a qualitative coincidence with the experimental evidence presented by Hertz & Hermanrud (1983).

The change of the surface gradient $\partial U/\partial r$ at $S_1$ (figure 9) shows that the viscous interaction between the dispersed phases is more significant at small values of $z$ and for a parabolic profile of outflow of phase 1. As for friction, it decreases with the increases of $z$ [this effect is caused by relaxation of the $U(r)$ profile].

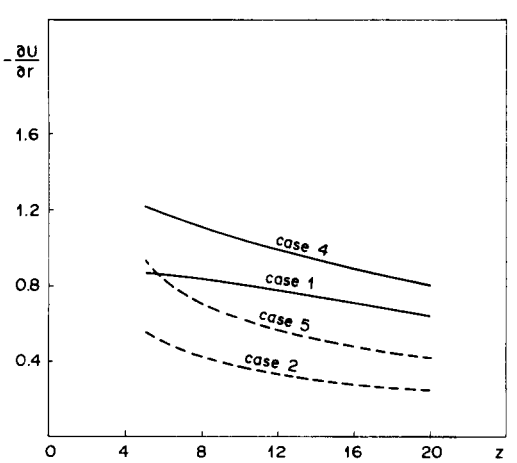


Figure 9. Variation of the axial velocity gradient at the interface of the dispersed phases.

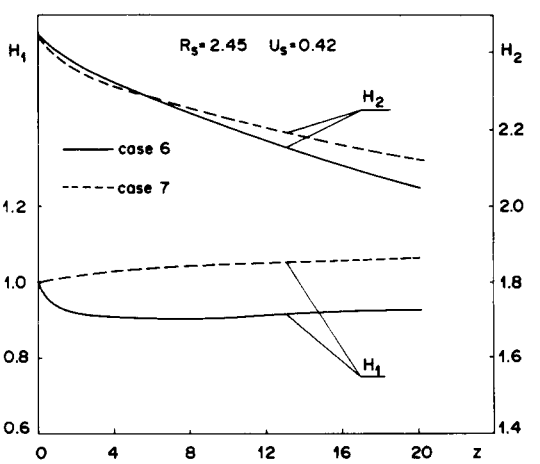


Figure 10. Effect of the $\mu_2/\mu_1$ ratio on the shape of the two interfaces.

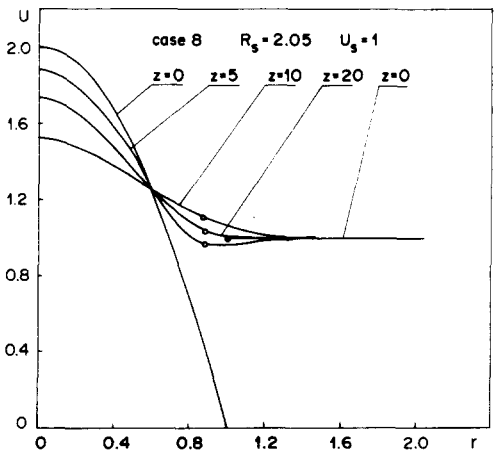


Figure 11. Effect of the parabolic initial profile of phase 1 on the axial velocity distribution.

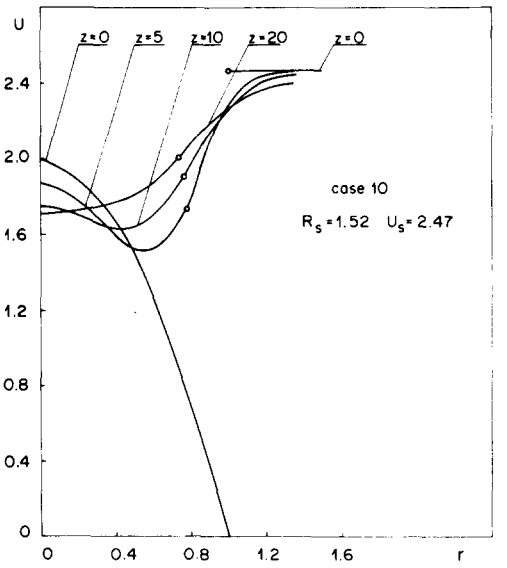


Figure 12. Effect of the outflow velocity $U_S$ on the axial velocity distribution.

Cases 6 and 7 are obtained from cases 1 and 2, although the dispersed phase 2 is water with an initial flow rate $Q_S = 75 \times 10^{-9}$ m$^3$/s while the average velocity of outflow is $u_S = 5$ m/s. The coefficients of surface tension are $\sigma_1 = 20 \times 10^{-3}$ and $\sigma_2 = 72 \times 10^{-3}$ N/m, respectively. What is worth noting here is that there is a difference between the viscosities of phase 1 and phase 2, $\mu_2/\mu_1 = 0.53$. The character of $H_1(z)$ and $H_2(z)$, shown in figure 10, is in agreement with the relations that have been disclosed. As compared to the previous cases, $H_2(z)$ decreases strongly because the acceleration of the concentric jet is stronger than the delay of phase 1. This effect, however, is caused by the difference between the viscosities.

What seems to be of interest is the case where both dispersed phases flow out with one and the same velocity. However, this is the way of obtaining cases 8 and 9, for which $u_P = u_S = 8.1$ m/s, while the rest of the parameters remain the same as in cases 4 and 5.

Results show that a total minimum occurs in the $U(r)$ profile for cross-sections that stay close to the nozzle exit (case 8). This is a result of the initial delay of the liquid layers of phase 1, the latter being close to the surface $S_1$. The delay, however, becomes smaller and smaller with increasing $z$ (figure 11).

Case 9 is not presented graphically, since, regardless of the fact that the compound jet consists of two different dispersed phases and $\sigma_2/\sigma_1 > 0$, the initial homogeneous velocity profile does not relax along $z$, while $S_1$ and $S_2$ remain cylindrical.

A better illustration of what has been stated is given in figure 12, which shows the variation of $U(r)$ for a number of cross-sections along $z$ (case 10). Case 10 differs from case 8 only with respect to the outflow velocity, $u_S = 20$ m/s. Here the effects of delay are strongly evident (figure 12).

## 5. CONCLUSION

The method presented provides the flow parameters of both the primary and concentric jet. One of its advantages exists in determining the characteristic equations of the interfaces (the radii of the primary and secondary compound jet surfaces). The second advantage follows from the possibility of studying the effects of interaction between two liquids through the inner interface.

The results illustrate the effect of the initial velocity profiles on both dispersed phases when they coincide and when they differ from one another. The effect of the difference

between viscosities has been revealed and the action of forces of interfacial tension upon surfaces $S_1$ (the central core) and $S_2$ (the compound jet) analysed. The distribution of the velocity axial component $U(r)$ has been obtained where a local minimum occurs. The effect of the velocity of outflow $u_S$ of phase 2 has also been studied.

The numerical method gives a solution of the case when the continuous phase 3 is considered to be a viscous fluid (i.e. a liquid).

## REFERENCES

BIRD, R. B., STEWART, W. E. & LIGHTFOOT, E. N. 1965 *Transport Phenomena.* Wiley, New York.

DUDA, J. L. & VRENTAS, J. S. 1967 Fluid mechanics of laminar liquid jets. *Chem. Engng Sci.* **22,** 855–869.

GOSPODINOV, P., RADEV, S. & PENCHEV, I. 1979 Velocity profiles and form of a laminar jet in immiscible liquid–liquid systems. *Int. J. Multiphase Flow* **5,** 87–99.

GOSPODINOV, P., LAZAROV, R. & RADEV, S. 1981 Numerical treatment of some problems of flow and instability of liquid jets. In *Mathematical Methods in Fluid Mechanics*; *Conf. Proc.*, Oberwolfach, F.R.G., pp. 79–93.

HERTZ, C. H. & HERMANRUD, B. 1983 A liquid compound jet. *J. Fluid Mech.* **131,** 271–287.

YU, H. & SCHEELE, G. F. 1975 Laminar jet contraction and velocity distribution in immiscible liquid–liquid systems. *Int. J. Multiphase Flow* **2,** 153–169.